The role of CD44 in periodontal ligament organization and repair

Holly Nicole Hinderberger

A thesis
submitted in partial fulfillment of the
requirements for the degree of

Master of Science

University of Washington
2012

Committee:
Tracy Popowics, PhD
Sue Herring, PhD
Richard Presland, PhD

Program Authorized to Offer Degree:
Oral Health Sciences

University of Washington

Abstract

The role of CD44 in periodontal ligament organization and repair

Holly Nicole Hinderberger

Chairperson of the Supervisory Committee:
Associate Professor, Tracy E. Popowics
Department of Oral Health Sciences

Periodontal ligament development and adaptation is fundamental for the proper function of dentition. The periodontal ligament (PDL) provides structural support for the teeth within the alveolar bone. Derived embryonically from the ectomesenchyme of the dental follicle, the PDL is a complex connective tissue composed of many cells including fibroblasts, macrophages, cementum cells, bone cells, as well as vascular and neural elements. The PDL is capable of high turnover rates as seen in orthodontic tooth movement. CD44, a multifunctional cell surface glycoprotein that is involved in cellular interactions, is thought to play an important role in the cellular organization of the PDL as well as in the migration of reparative cells after PDL injury. The purpose of this study was to determine the significance of CD44 during normal PDL adaptation and during PDL repair in response to orthodontic injury. At 41 days postnatal (dpn) four wild-type and four CD44 knockout mice were sacrificed and prepped for histological analysis. Histological sections were prepared and analyzed using Canvas software. Fibroblast cell angles were measured with respect to the root surface 20 μm below the cementoenamel junction (CEJ). A previous study found a significant difference between the PDL

fibroblast angle measurements of CD44 knockout and wild-type mice at day 26 dpn; however, no significant difference was noted at day 41 dpn. This finding suggests that the lost function of CD44 is capable of correcting itself in the CD44 knockout mice, or that there are other receptors found in the PDL, such as RHAMM, that compensate for the function of the CD44 receptor. In order to explore the significance of CD44 in PDL repair after orthodontic tooth movement an orthodontic wire was placed unilaterally on the maxilla of 21 wild-type and five CD44 knockout mice at day 31 dpn. Wires were activated for 5 days before being cut to allow for recovery. Mice were sacrificed at day 41 dpn and prepped for histological analysis. Results of this study are to be determined.

TABLE OF CONTENTS

LIST OF FIGURES

LIST OF TABLES

ACKNOWLEDGEMENTS

This thesis would not have been possible without the help and support of many people within and outside of the University of Washington community. Dr. Tracy Popowics, my mentor and friend, provided a positive environment for me to learn and explore the world of dental research. Her compassion and understanding are traits that I hope to mirror in my future endeavors. The advice and information shared among my committee from Dr. Susan Herring and Dr. Richard Presland were invaluable. A special thanks is extended to Dr. Siddharth Vora for helping me with the orthodontic procedures. Dr. Vora also deserves many thanks for being patient with me while I anxiously awaited every mouse to wake up from the anesthesia during our long procedure days. A heartfelt thanks goes to Xian Bai for her countless hours of sectioning and for providing me with beautiful slides to analyze. I feel so lucky to be surrounded by such wonderful and intelligent colleagues and professors at the University of Washington. Your friendship and support has been crucial to my success and I value each of your friendships.

To my family, your support and love has gotten me to where I am today. The amount that I appreciate all you have done for me is limitless. To my mother, Carolyn, and my father, Ron, you have always encouraged me throughout my education and shown me the value of determination and hard work. Thank you for always believing in me, especially when I doubted myself.

This research was also made possible by the Dr. Douglas L. Morell Research Fund grant.

DEDICATION

This thesis is dedicated to my experimental mice, without which this research could not be completed.

I would also like to dedicate this thesis to all students pursuing a career in dentistry. Continue to follow your dreams.

Introduction

The periodontal ligament is an important part of the dentition. It provides an extensive support network for the tooth and is composed of many cells that offer a variety of functions such as attachment and the production of new tissue. Attachment cells, such as fibroblasts, aid in the production of a collagen network that adheres to the root of the tooth on the cementum surface to the surrounding alveolar bone. Fibroblast function is important to ensuring that the tooth remains anchored properly within the tooth socket to allow for accurate mechanotransduction. There are cell receptors located on the surface of fibroblasts, along with many other cells, that play a role in the regulation of these cells. One such receptor is the CD44 cell surface receptor. Previous studies have demonstrated that the CD44/fibroblast role is important in the development and repair of heart, lung, skin and periodontal tissues in response to injury. This study will aim to show the relationship between CD44 and fibroblasts during the development of the periodontal ligament as well as the adaptation of this important connective tissue after orthodontic injury.

CHAPTER I: Literature Review

The periodontal ligament

The periodontal ligament (PDL) develops during tooth eruption and provides structural support to the dentition. Embryologically, the PDL is derived from the ectomesenchyme of the dental follicle, which surrounds the tooth as it develops. As the tooth erupts, collagen fibers transition from an orientation parallel to the root surface to more perpendicular and oblique orientations. Specifically, dental follicle cells give rise to the PDL fibroblasts that begin secreting collagen. These collagen fibers are continuous with Sharpey's fibers extending from the surface of both the adjacent bone and the cementum of the tooth and form the tooth attachment. As the periodontal ligament forms at the cementoenamel junction the fibroblast and collagen cells begin to organize perpendicular to the root surface and in an apical direction in response to the establishment of occlusion. Once in occlusion, the periodontal ligament continues to form through the proliferation of ligament fibroblasts and the production of collagen. During normal occlusion, cusp morphology directs tooth contact causing the tooth to move within its socket in many different planes. The magnitude, direction, duration and frequency of occlusal forces initiate adaptive remodeling of the ligament; however the mechanism of ligament responsiveness to load is unclear (Berkovitz et al., 1982). In this study I will investigate how the PDL adapts to loading changes and initiates a remodeling response as the tooth erupts into occlusion.

The periodontal ligament, like other connective tissues, consists of many different cells as well as extracellular fibers and a collagenous extracellular matrix. Fibroblast cells are in the highest abundance and are involved in the high turnover rates of proteins within the extracellular space, namely collagen. Additionally, PDL fibroblasts have a prominent actin network associated with the cytoskeleton. Fibroblast cells organize along the direction of the collagen fiber bundles with processes that wrap around the continuously remodeling fibers. Due to the high rate of turnover occurring within the periodontal ligament, interferences, such as periodontal disease or injury, can disrupt fibroblast function and result in a rapid loss of the supporting tissue (Lekic et al. 1996). This study will also investigate mechanisms of ligament repair, such as cellular repopulation of the injury site.

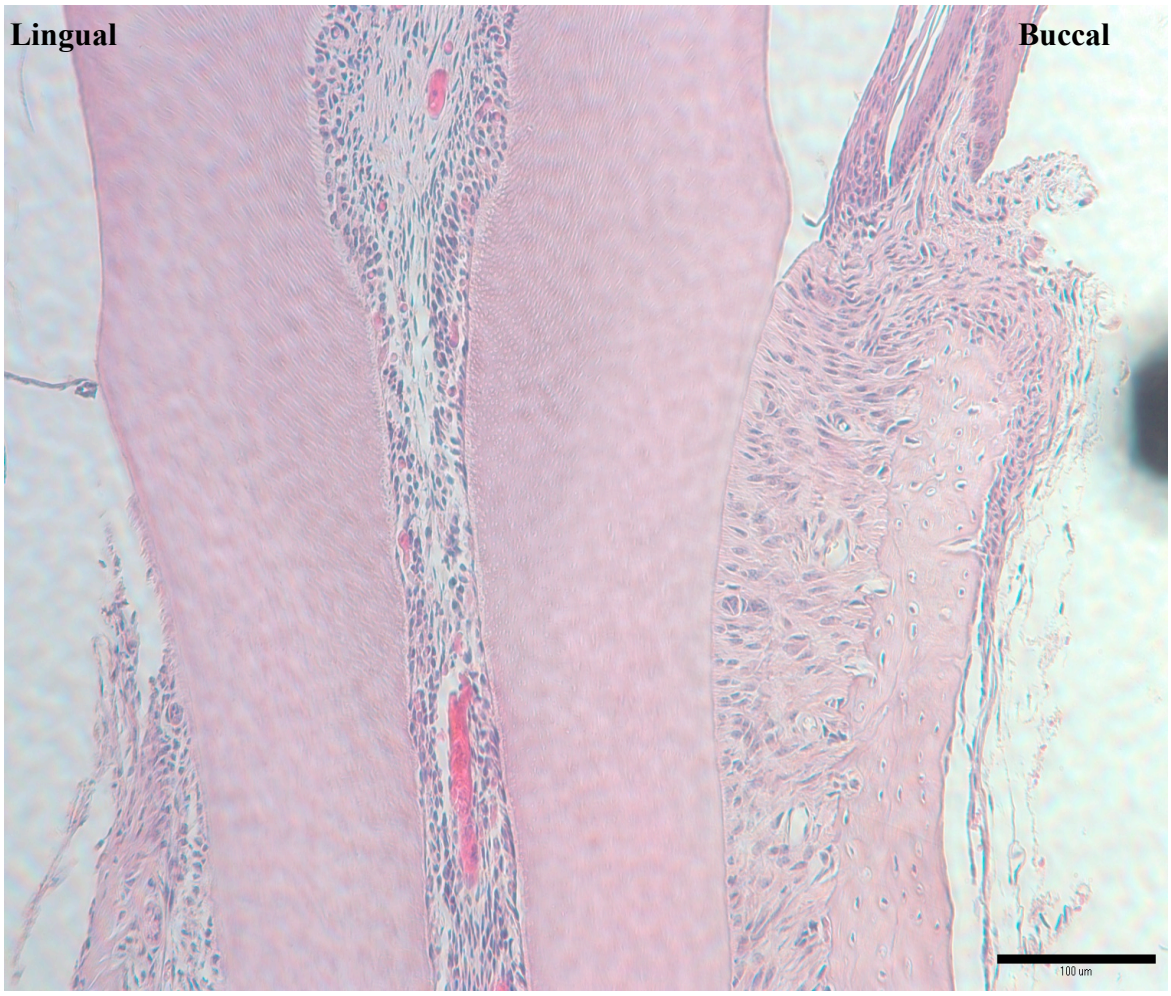

Figure 1: The Periodontal Ligament. Coronal section of the first molar in a wild-type day 41 dpn mouse. Image magnification: x20. Note the organization of the cells and collagen bundles in the cervical region of the PDL, specifically on the buccal side.

CD44

The role of the CD44 receptor in PDL adaptation and healing is the focus of this study. CD44 is a multifunctional glycoprotein located on the surface of many cells. CD44 is involved in cell-to-cell and cell-to-matrix interactions as well as cellular migration and adhesion. Some important roles of CD44 include cellular trafficking, uptake and degradation of hyaluronic acid, as well as cell signaling for hematopoiesis and apoptosis (Naor et al., 1997). CD44 is a single chain molecule with an extracellular domain, which contains the ligand-binding sites, a membrane region, which binds extracellularly to cell membranes, a transmembrane-spanning domain, and a cytoplasmic tail. The principal ligand for the CD44 receptor is hyaluronan or hyaluronic acid (HA). Additional ligands include fibronectin, osteopontin and laminin. The molecular sequence of CD44 has displayed high interspecies homology and is expressed in a large number of mammalian cell types including PDL fibroblast cells, adult stem cells, mesenchymal stem cells, osteoclast cells, and osteoblast cells (Häkkinen et al. 1993). The standard CD44 isoform (CD44s), which is expressed in most cell types, is comprised of exons 1-5 and 16-20. Splice variants that contain different exons are designated CD44v. Alternative splicing, while it is responsible for structural and functional diversity, has also been linked to tumor metastasis (Naor et al. 1997).

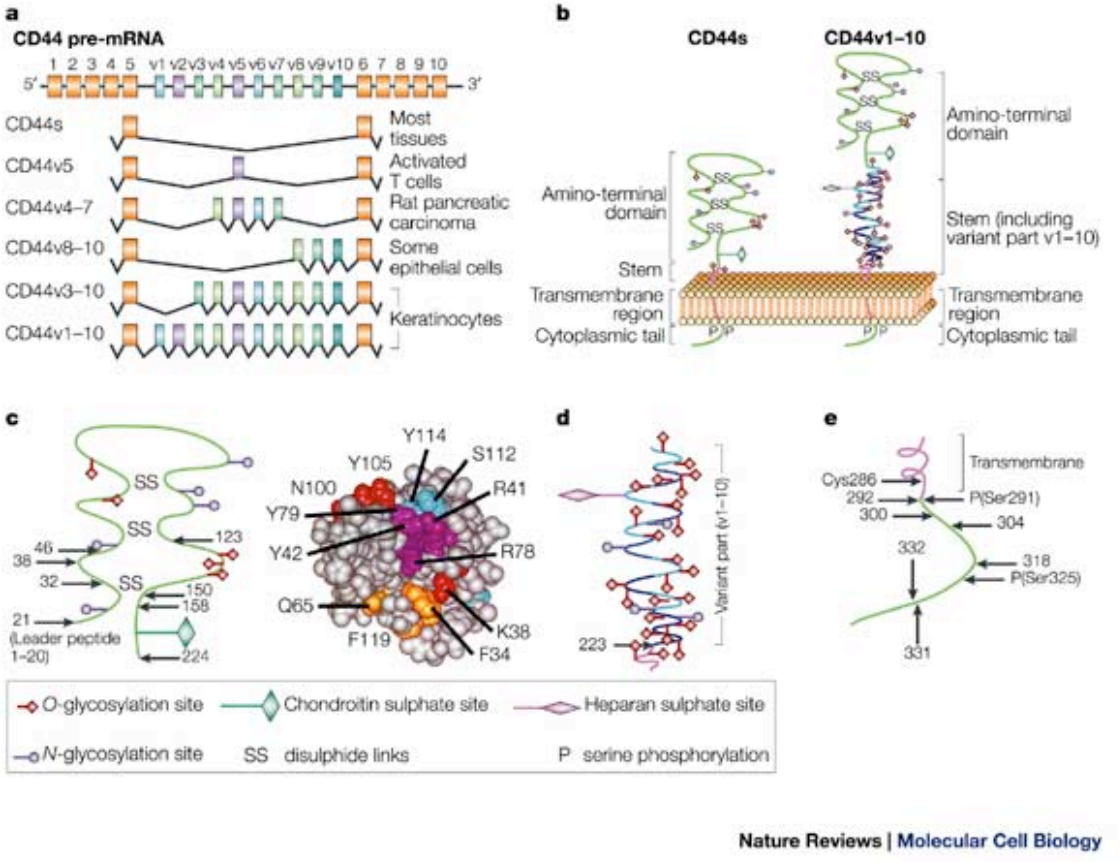

Figure 2: CD44. A. CD44 pre-mRNA. B. Protein structure of CD44 standard (smallest isoform) compared to CD44v1-10 (largest isoform). C. The amino-terminal domain of CD44 contains the hyaluronan-binding motifs. The three highly conserved cysteine residues that are key in the stability of the link module are shown on the left. The image on the right depicts a possible three-dimensional structure. Marked amino acids indicate those that cause loss of hyaluronan binding upon mutation. D. Stem structure of CD44s, consisting of 46 amino acids. E. The carboxyl-terminal of CD44 is involved in cytoskeletal organization and signaling (Ponta et al., 2003).

A previous University of Washington study comparing PDL development in CD44 knockout mice to wild-type mice suggested that the CD44 receptor might be involved in periodontal adaptation to occlusal loads. CD44 knockout mice were obtained with complete abolishment of all CD44 isoforms via changes to the exons encoding the invariant N-terminus. This project tested both CD44 knockout mice and wild-type mice specifically comparing the progress of development histologically at developmental stages including 18 and 26 postnatal days (Boyd 2010 SURF). The histology revealed no significant difference in the orientation of fibroblast cells in the CD44 knockout mice during development of the PDL at 18 days dpn and earlier. Fibroblast orientation was noticeably different, however, in wild-type vs. knockout mice at day 26 dpn during the onset of occlusion. At this time point the average angle of a wild-type PDL fibroblast relative to the root axis was 91.7º whereas for a CD44 knockout animal this measurement was 116.0º. This suggests that CD44 could possibly play a role in the organization of the periodontal ligament under occlusal stress rather than during development. In my study we will verify the importance of the CD44 receptor in PDL adaptation to occlusal loads through comparison of fibroblast cell orientation at a later occlusal stage, day 41 dpn.

Orthodontic tooth movement

Orthodontic treatment is a common and simple source of injury that is of interest to my study. Hyalinization describes the loss of cells from an area due to necrosis and is an important component in the tooth movement process (Rody et al., 2001). Orthodontic

tooth movement is driven by pressure and tension. On the pressure side, bloodflow is disturbed in the PDL, which is compressed. Cell death occurs in the compressed site, and macrophages begin to resorb the hyalinized tissue since tooth movement cannot occur until the necrotic tissue is removed. Simultaneously, bone resorption is occurring in the alveolar bone socket along the pressure side, ultimately leading to tooth movement through the socket (von Böhl et al., 2008). The origin of osteoclasts into the hyalinized site is unclear and there are many interpretations as to where they originate. These interpretations include: the cells are macrophages or other cells located in the site, osteoclast predecessors are circulating monocytes, or that these osteoclasts originate from the same progenitor cell, which develop into mononuclear phagocytes or osteoclast progenitors in hematopoetic tissues (Rody et al., 2001). On the tension side the PDL is stretched and bloodflow is activated, which promote osteoblast activity along with osteoid deposition, leading to mineralization (von Böhl et al., 2008). When the tooth reaches the desired place in occlusion periodontal remodeling and repair occurs to maintain the structure and stability of the tooth within the socket.

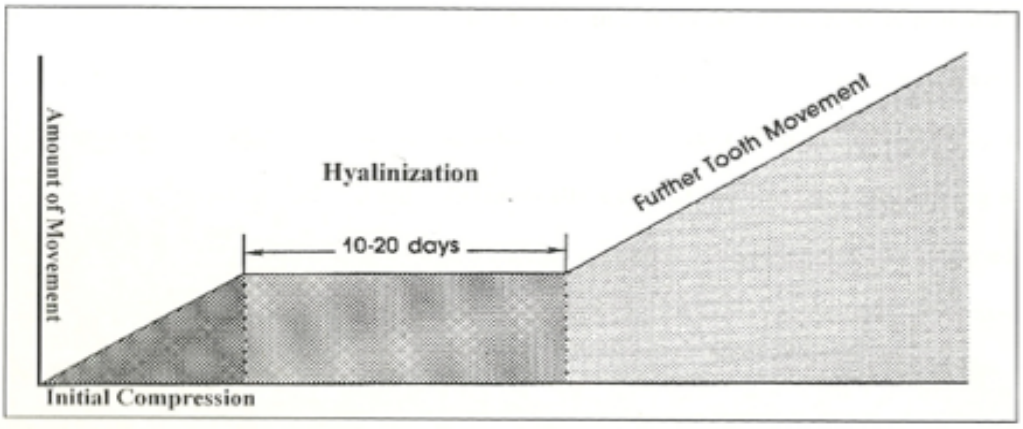

Figure 3: Orthodontic Tooth Movement Over Time (Ten Cate, 2008).

CD44/HA binding is expected to promote PDL fibroblast migration in association with periodontal tissue repair, such as in orthodontically induced PDL injury. CD44 and hyaluronan have been found to localize in epithelial tissues during specific repair stages. In 1-day-old epithelial wounds the first migrating cells exhibited low levels of the CD44 receptor. In 3-day-old wounds the migrating cells as well as the newly formed granulation tissue clearly expressed heightened levels of CD44 and hyaluronan (Naor et al., 1997). We will use this data to extrapolate information regarding the response of PDL cells after similar injuries. These previous results suggest that, if this pattern continues, at 5 days post-treatment, heightened levels of CD44 expression are expected to occur in wild-type mice compared to the CD44 knockouts emphasizing the role of the CD44 receptor in PDL recovery. CD44 is expected to increase cell migration and fiber formation in the PDL in response to injury or infection by upregulating cell to cell and cell to matrix adhesions. As the periodontal ligament begins to heal, many new PDL cells are recruited to the site of injury to restore the structural integrity of the tissue. New cells can be recruited through surrounding blood vessels as well as progenitor cells in the surrounding area (Lekic et al., 1996).

The function of CD44 in cellular migration has been studied in a variety of other tissues including the lung and heart. A study performed in 2008 compared the cytoskeletal architecture and migration of lung fibroblasts within CD44 deficient and wild-type mice (Acharya et al. 2008). This study concluded that CD44 deficient animals exhibited a reduction in components of cell movement; for example, fewer stress fibers and focal adhesions, than their CD44 wild-type counterparts. Additionally, CD44 deficient fibroblasts experienced a higher rate of migration but lacked the ability to orient

toward the wound site; thus the recruitment of fibroblasts to injury sites was found to be CD44 dependent. A further study from 2008 investigated the role of the CD44 receptor in infarct healing of murine cardiac tissue (Huebener et al. 2008). Inflammation typically increases at a steady rate after trauma as mesenchymal cells infiltrate the site of injury for repair. In comparison with wild-type mice, CD44 knockout mice showed an enhanced inflammatory phase marked by prolonged neutrophil and macrophage infiltration during wound healing. Furthermore, the CD44 knockout mice showed a decrease in fibroblast infiltration. These findings lead me to believe that the CD44 receptor may play an important role in the recruitment of additional PDL fibroblasts to a periodontal wound site for tissue repair.

CHAPTER II: Research Design

Approach

C57BL/6J mice were separated into two different studies. In the first study, four CD44 knockout mice day 41 dpn and four wild-type day 41 dpn mice were used to analyze the normal remodeling that takes place after adult molars come into occlusion and begin PDL mechanotransduction. Young mice were weaned at day 23 dpn and were given a soft protein gel to supplement the laboratory chow. By day 30 dpn mice were given only solid food in order to allow newly erupted teeth to adapt normally. CD44 knockout mice were provided through the Ontario Cancer Institute. All known isoforms of CD44 were abolished for the preparation of CD44 mutant mice by eliminating the exons that encode the invariable N-terminus region.

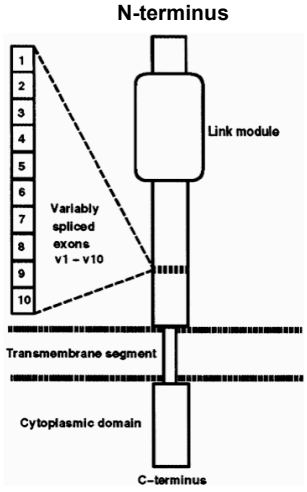

Figure 4: Simplistic Model of the CD44 Transmembrane Molecule. All CD44 isoforms were abolished in the creation of CD44 knockout mice by removing the exons which code for the invariable N-terminus domain seen above (Bajorath, 2000).

Mice in this study were raised under normal conditions until sacrifice at day 41 dpn. At sacrifice, mice were decapitated with complete removal of the mandible in preparation for the histomorphometric analysis. The second study, in collaboration with Dr. Zee Liu and Dr. Siddharth Vora from the department of Orthodontics, sought to develop a protocol to determine cellularity within the PDL during recovery after orthodontic trauma in CD44 knockout and wild-type mice. Mice were weaned in the same way as those used for the first study. At day 31 dpn, 21 wild-type and five knockout mice were anesthetized so that activated orthodontic wires could be placed unilaterally on the maxilla suggested by the method proposed by Dr. Zi-Jun Liu (Liu et al., 2005). During the five-day experimental phase during which the orthodontic wires were activated, mice were placed on a strict soft food diet consisting of protein gel and watered down laboratory chow. At day 36 dpn, mice were anesthetized in order to facilitate the removal of the orthodontic wires and BrdU injections to be administered. During the five-day recovery phase mice were placed back on the normal hard food diet of laboratory chow. Mice were sacrificed at day 41 dpn and decapitated and dissected for histomorphometric analysis.

Figure 5: Mouse Skull. Adult CD44 knockout mouse.

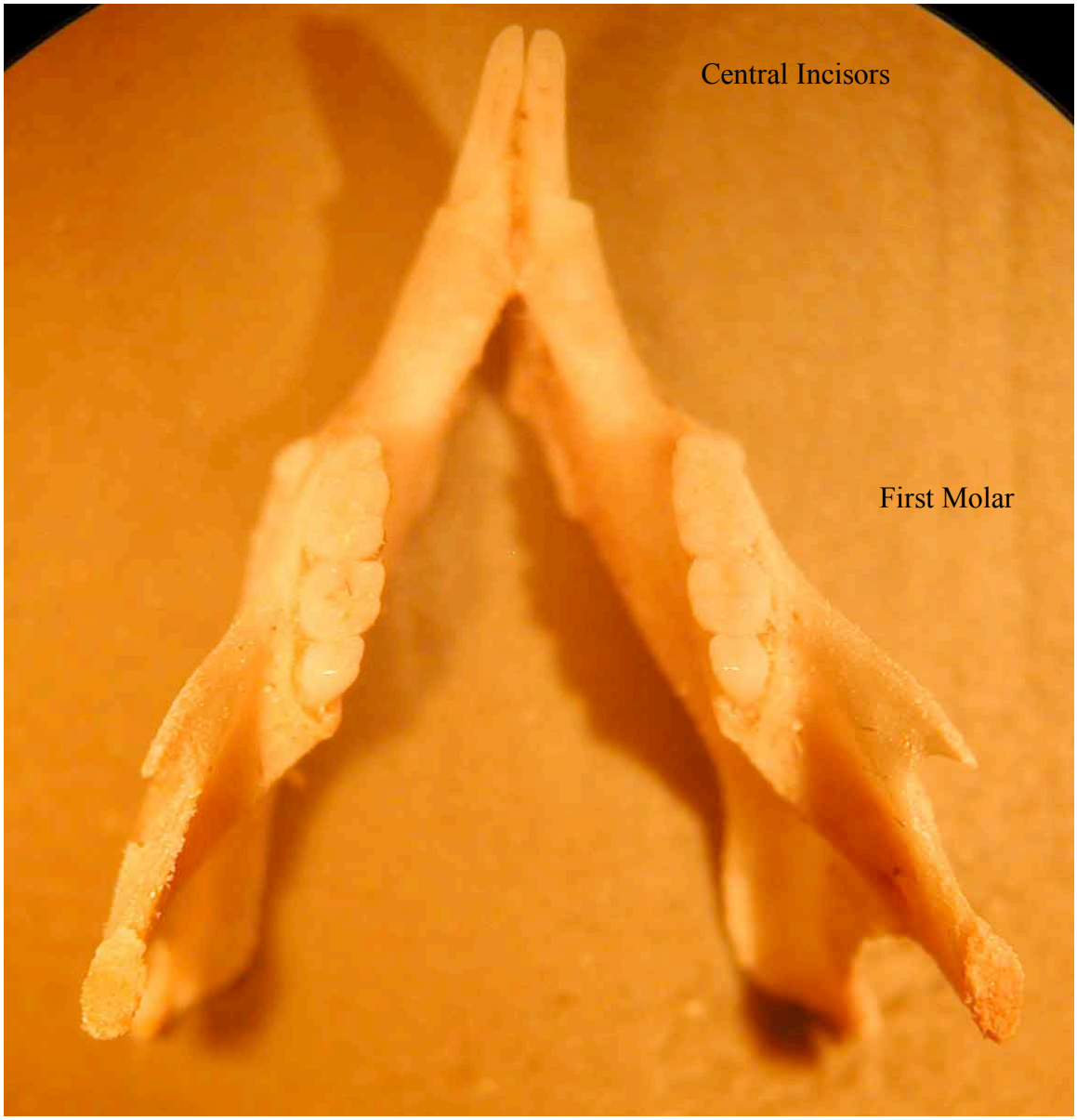

Figure 6: Mouse Mandible. Adult CD44 knockout mouse.

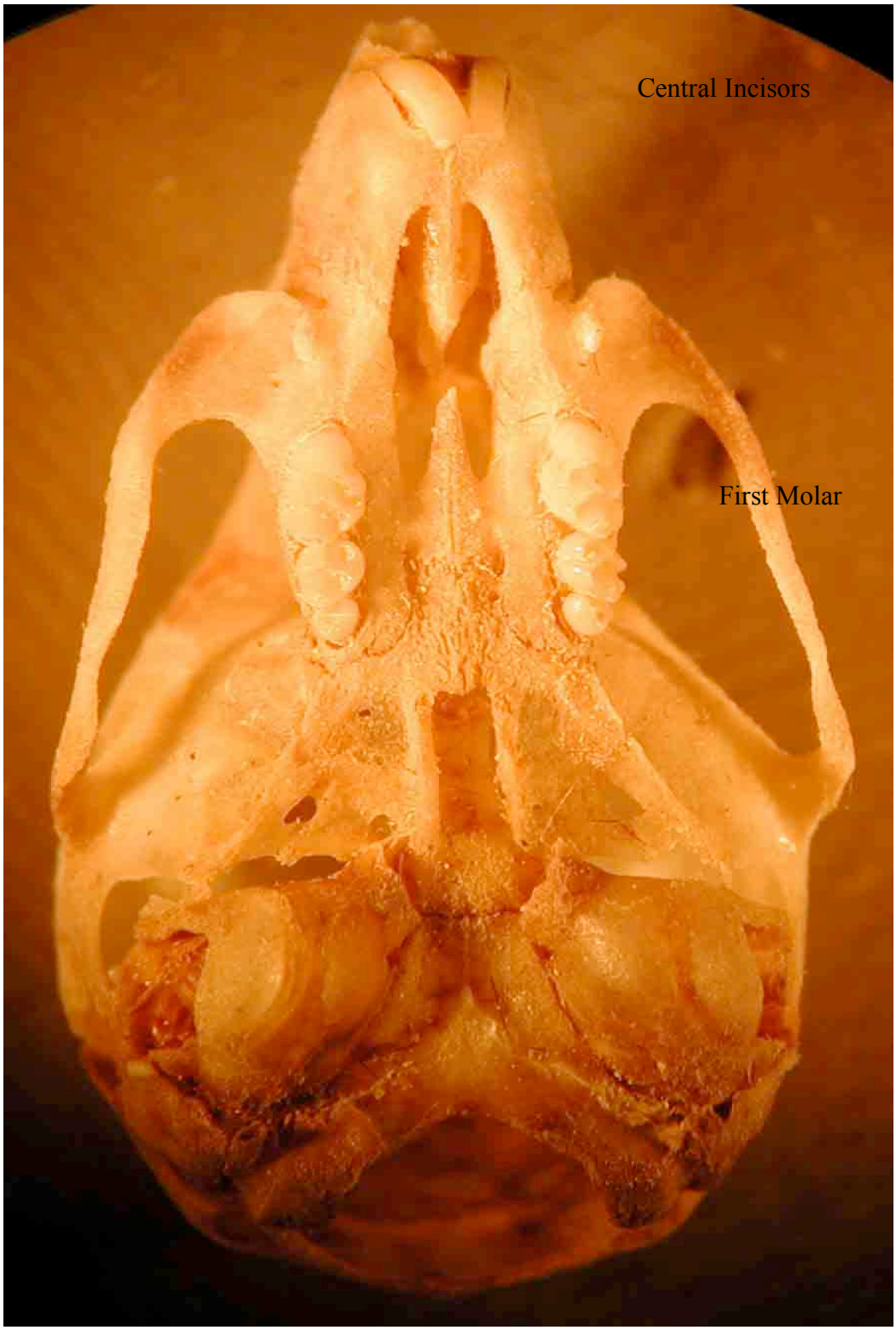

Figure 7: Mouse Skull-Palatal View. Adult CD44 knockout mouse.

Hypothesis

This study will investigate the general hypothesis that CD44 expression on PDL fibroblasts is involved in fibroblast organization and migration, and that the absence of the CD44 receptor will result in differences in PDL organization and post-injury cellularity. This study will be divided into an investigation of periodontal organization during occlusion, as well as PDL response to injury with orthodontic treatment. A mouse model will be used to compare the mesial buccal root of the first molar in CD44 wild-type and CD44 knockout mice. This will be examined using the following specific aims:

Specific Aim One: To analyze whether the PDL of CD44 deficient mice will exhibit a difference in the orientation and organization of associated fibroblast cells in response to newly acquired occlusal loads as compared to a wild-type control.

We hypothesize that the mutant strain will exhibit less structural integrity and a difference in structural organization within the PDL as seen in a greater variation in PDL fibroblast orientation in knockout mice versus the wild-type controls. When comparing the PDL of the first mandibular molar in mice with the CD44 receptor to those without the receptor I expect to see greater disorganization of the fibroblasts in CD44 KO mice. I expect both groups to have similar densities of fibroblast cells and collagen fibers in the PDL because there will be no trauma inflicted on the PDL, in contrast to the orthodontic treatment seen in specific aim two. Since the CD44 receptor plays a role in cell-matrix interactions, I expect it to be active in cell establishment and orientation in response to mechanical loading. Thus, the orientation of the fibroblasts will be consistent in the wild-

type strain since CD44 will be active in development, whereas the mutant strain will exhibit greater variation in cell orientation.

Specific Aim Two: To develop a successful protocol to determine cellularity and investigate the role of the CD44 in the migration of periodontal fibroblast cells to sites of orthodontic injury.

In order to ultimately analyze the role of CD44 signaling in the PDL following orthodontic injury a successful and efficient protocol was needed using a mouse model. We predict that in the absence of CD44, PDL cells will be unable to infiltrate the wound for tissue repair. In order to investigate this ultimate issue, it is necessary to have a reliable model for injury and repair of the PDL. This will be undertaken using excess orthodontic force. We predict the wild-type strain to exhibit normal PDL repair, whereas PDL recovery in the mutant strain will be impaired and exhibit a difference in the cellularity of the affected site. When the orthodontic wire is activated, injury will occur to the PDL of the maxillary molars. A successful outcome would be hyalinization in the area where the PDL is injured from the movement of the tooth enforced by the orthodontic wire. The center of rotation, located approximately one-third down the tooth root, is the point at which rotation occurs when a tooth is being moved, for instance, with an orthodontic wire (Brooks et al., 2009). As the wire rests on the buccal crown of the molars the force will cause the crown to tilt lingually causing hyalinization to occur in the lingual gingival and alveolar crest fiber regions. As the cervical region moves lingually the root apex will move buccally causing hyalinization in the apical region of the buccal PDL.

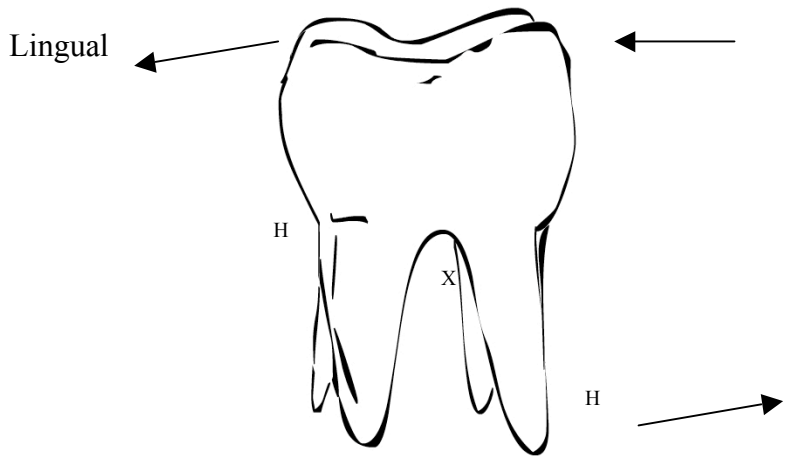

Figure 8: Tooth Movement and Hyalinization. Molar tooth cartoon showing the presumed direction of tooth movement in response to the orthodontic treatment. X: Center of rotation. H: Areas of hyalinization.

After the wire is clipped, during the healing period, the PDL of the wild-type mice should exhibit an increase in the number of fibroblasts in order to undergo injury repair, shown by higher cellularity within the PDL when compared to the CD44 knockout mice. The mice that lack the CD44 receptor will have fibroblasts with impaired migration, therefore an inability to home toward the wound site, exhibiting low PDL cellularity. BrdU staining will be used to provide information regarding cellular activity; cells that stain brown are BrdU+ and actively dividing.

CHAPTER III: Methods

Animal Manipulation

Specific Aim One

In order to determine differences in fibroblast orientation during PDL development between CD44 knockout and wild-type mice, sample sizes of 4 mice were collected. Mice were housed in plastic cages and given a diet composed of ground laboratory chow, water. They were also on a 12-hour light/dark cycle. Mice were weaned from their breeding pairs at day 23 dpn and separated based on gender. To ensure weaning success mouse pups were given the ground laboratory chow supplemented with a soft diet consisting of a protein gel. The soft food protein gel was provided for seven days after being weaned, upon which only solid food was given in order to allow newly erupted teeth to adapt normally. At day 41 dpn the mice were sacrificed, decapitated and placed in Bouins fixative overnight to preserve the tissue. At this age the upper first molar has fully erupted. After 24 hours in the Bouins fixative, the skulls were dissected and the mandibles were cut symmetrically between the two central incisors. Left and right mandibles were labeled and placed in tissue cassettes. An acetic acid-formaldehyde-saline (AFS) solution was prepared for the decalcification process. Tissue cassettes were submerged in AFS, sealed with parafilm, and placed in a refrigerator to begin the decalcification process. The AFS solution was changed every 48 to 72 hours for 10 days to ensure complete decalcification in preparation for sectioning.

Following the 10-day decalcification process the tissue cassettes were processed using a Miles Scientific Tissue-TEK VIP tissue processor in order to remove excess water and replace it with paraffin wax so to produce thin sections. The tissues were processed during a 16-hour cycle of alcohol and paraffin wax washes. Following tissue processing the tissues were embedded in hot paraffin wax using a Reichert-Jung Tissue Embedder. Paraffin blocks were given sufficient time to cool and solidify prior to beginning the sectioning process.

Specific Aim Two

In order to determine differences in fibroblast migration and adaptation after PDL injury, 21 wild-type and five CD44 knockout mice were used to develop a successful protocol for orthodontic manipulation. Mice in this study followed the same care protocol as described above including living environment and weaning procedure. At day 31 dpn the mice began orthodontic treatment. Weights were recorded and mice were anesthetized via intraperitoneal injections of Ketamine (87 mg/kg) and Xylazine (13 mg/kg). Animals were laid on their backs on a head holding device that kept their limbs secure while the orthodontic wires were placed. The restraining device consisted of a plastic base (6.5 x 9 inch) with two vertical pillars used to restrain limbs of the mice according to a protocol from Rody et al. Thread was used to restrain the limbs and to hold the mouth open by the mandible. An orthodontic wire was placed on the right maxillary molars and secured around the central incisors with a loop and adhesion. Once the loop adhesive was cured the wire was activated and brought back across the molars, through the diastema, to rest buccally along the molars. After wire activation the mice were brought back to the animal facility and were put on a strict soft food diet.

Intraperitoneal buprenorphine (0.05 mg/kg) injections were given every 12 hours following wire activation for 2 days after the procedure. Mice were also monitored daily with weight recordings and notes. At day 36 dpn mice were anesthetized with the same mixture described above. Once anesthetized, orthodontic wires were clipped at the loop attached to the incisors. After the wire was clipped subcutaneous injections of BrdU (0.1 mg/gm) were administered for later immunohistochemistry analysis. The five-day activation period was determined according to previous experiments using a rat model (Okafuji et al., 2006). A five-day recovery period followed the activation phase. This time period was used for convenience and to maintain a symmetrical experimental timeline. Mice were sacrificed at day 41 dpn and followed the same procedure as described above.

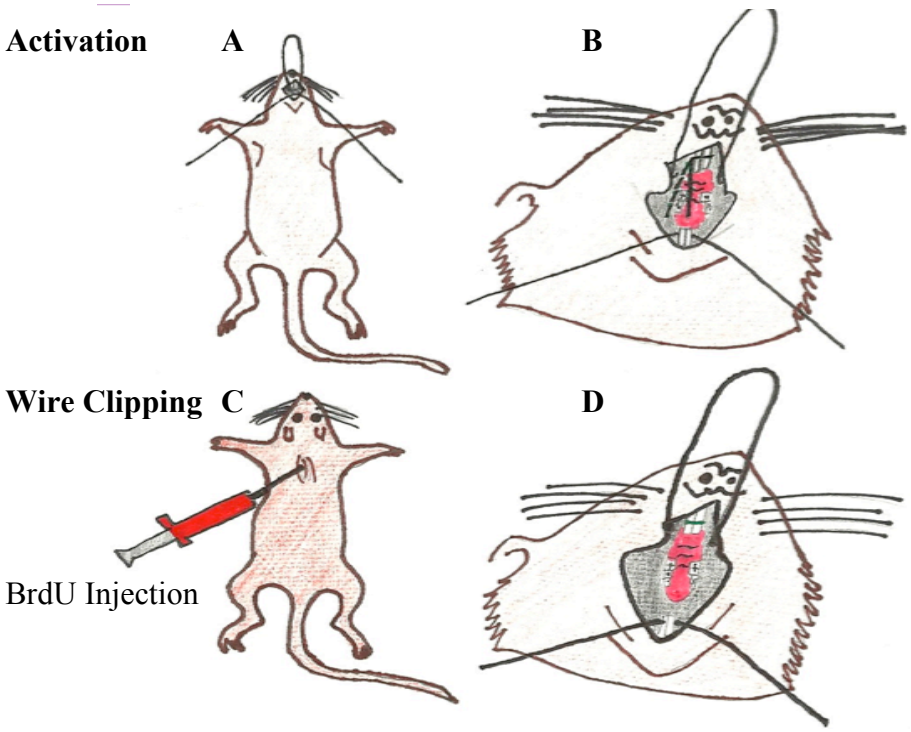

Figure 9: Orthodontic Manipulation. Wire activation occurred at 31 dpn. A: Mice were anesthetized and secured using thread. B: Close up image of the mouth of the mouse during orthodontic wire placement and activation. Wires were cut and removed at 36 dpn. C: Mice were anesthetized and subcutaneous injections of BrdU were administered. D: Close up image of the mouth of the mouse during wire removal.

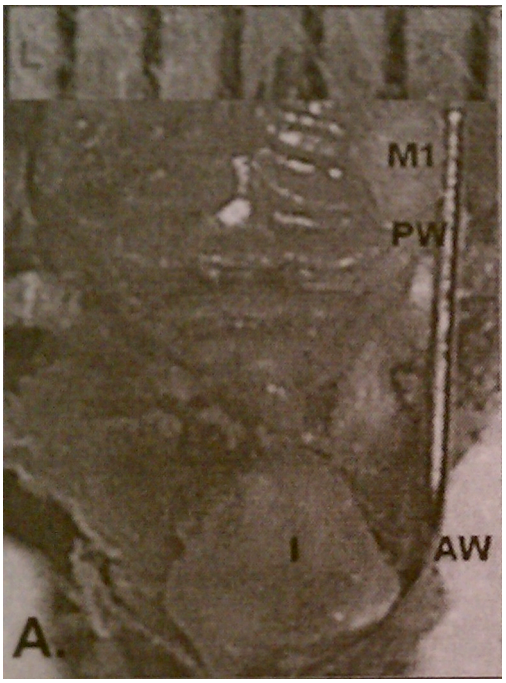

Figure 10: Orthodontic Wire Placement. AW: Anterior wire (anchorage section). PW: Posterior wire (active section). M1: First molar. I: Upper incisor. L and R: Left and Right (Vora, 2011).

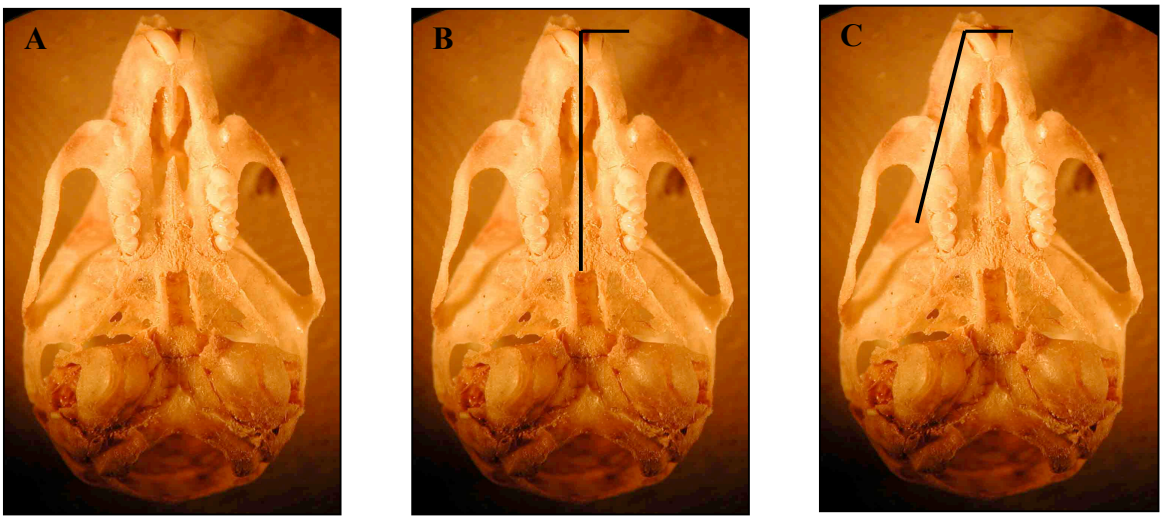

Figure 11: Orthodontic Wire Activation. A: Adult CD44 knockout skull, palatal view. B: Initial wire placement for securing purposes. C: Wire in the activated state.

Staining Techniques

Tissue section collection and staining were identical between both studies. The paraffin-embedded tissues were sectioned coronally, along the mesial buccal root of the first molar. Sections 5 μm in thickness were collected using a Reichert-Jung Biocut 2030 rotary microtome and placed in a warm water bath before being mounted on precoated slides for analysis. Sections were collected throughout the entire first molar and specimens clearly showing the entire length of the mesobuccal molar root were selected for staining. Selected slides were placed on a slide warmer overnight in preparation for staining. A hematoxylin and eosin stain (HE) was performed on the tissue slides according to the following protocol:

1. 100% Clearene for 5 minutes
2. 100% Clearene for 5 minutes
3. 100% Ethanol for 3 minutes
4. 90% Ethanol for 3 minutes
5. 80% Ethanol for 3 minutes
6. 70% Ethanol for 3 minutes
7. Water Flowing for 2 minutes
8. Hematoxylin for 30 seconds
9. Water Flowing for 10 minutes
10. Eosin for 4 minutes
11. Water Flowing for 2 minutes
12. 70% Ethanol for 3 minutes
13. 80% Ethanol for 3 minutes
14. 90% Ethanol for 3 minutes
15. 100% Ethanol for 3 minutes
16. 100% Clearene for 5 minutes
17. 100% Clearene for 5 minutes

Aluminum ions and hematoxylin form a complex called hemalum, which colors the nuclei of cells along with keratohyalin granules a dark blue color. The counterstain of eosin is composed of an alcoholic solution that stains eosinophils and other structures in

shades of red and pink. Following the staining process slides were given time to dry before adding cover slips.

Data Collection

Specific Aim One

Once the histology slides were prepared, a Nikon Eclipse E400 microscope was used to select specific slides for analysis. Three consecutive tissue sections were selected for measurement. Images of the slides were taken using a SPOT camera on the microscope and imported into Canvas software for measurement. Images were calibrated and a uniform box (55 μm x 30 μm) was drawn for analysis. The box was placed 20 μm below the cementoenamel junction (CEJ). This region containing the alveolar crest fibers encounters the highest stress loads during mecanotransdunction following eruption therefore provides strong evidence for comparison between PDL fibroblasts in wild-type and CD44 knockout animals (Kaewuriyathumrong et al., 1993). A line was drawn from the top of the surrounding alveolar bone to the point indicated 20 μm below the CEJ. This line provided a consistent way to orient the analysis box. The analysis box was placed along the line spanning the PDL equidistant between the alveolar bone and the root of the first molar. Once the box was in place fibroblasts entirely contained within the box showing clear directionality were marked for further measurement. Straight lines spanning the entire length of the selected fibroblasts were drawn. Additionally, a line from the CEJ down the length of the cementum was drawn for angle measurements. Using the Canvas angle measuring software, each marked fibroblast was measured with

respect to the cementum. Angles were noted in an excel spreadsheet for later statistical analysis.

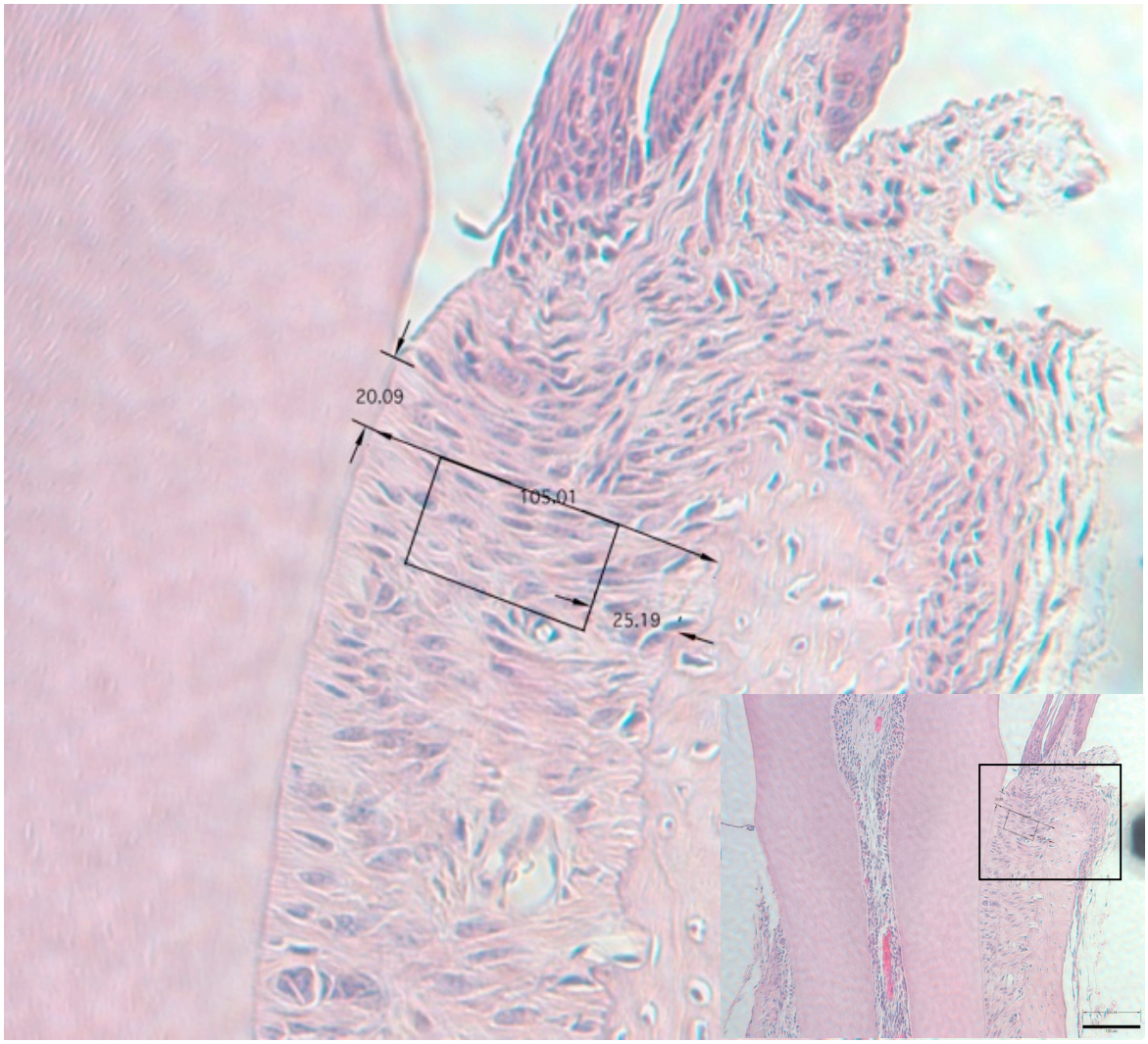

Figure 12: Wild-type Canvas Image. Coronal section taken from the first molar of a wild-type day 41 mouse at x20 magnification. Alveolar crest fiber region is shown within the measurement box.

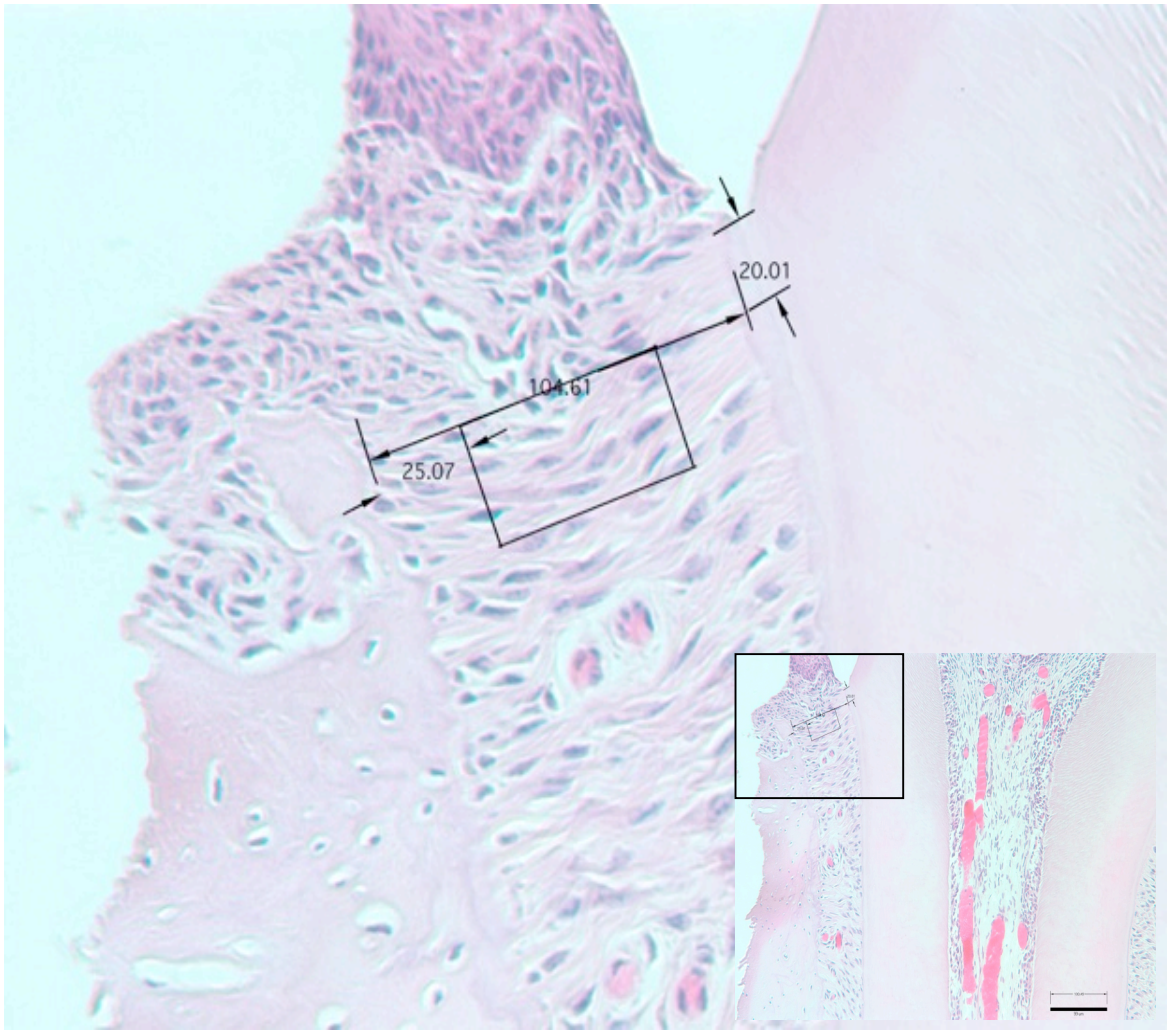

Figure 13: CD44 Knockout Image. Coronal section taken from the first molar of a CD44 knockout day 41 mouse at x20 magnification. Alveolar crest fiber region is shown within the measurement box.

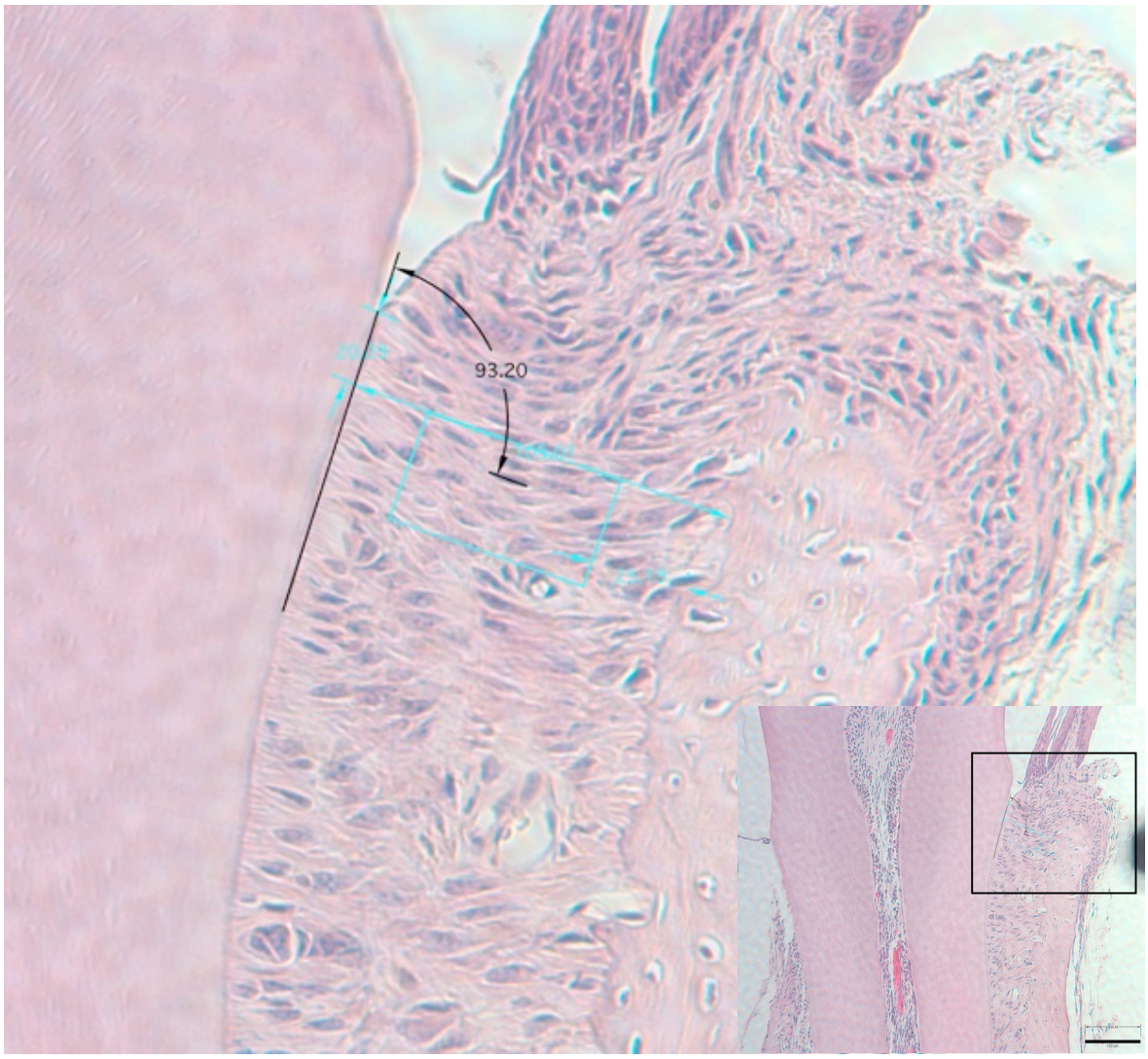

Figure 14: Angle Measurement Example. Coronal section taken from the first molar of a wild-type day 41 mouse at x20 magnification. Alveolar crest fiber region is shown within the measurement box. Fibroblast cells displaying clear directionality were measured with respect to the cementum of the tooth.

Statistical Analysis

Since the data collected were values representing angle measurements, a Watson-Williams F-Test from Oriana was used to analyze data collected from the histology slides. The Watson-Williams test analyzes the equality of the means of two or more samples.

Data from each slide were imported into the software and a vector mean and circular standard deviation was calculated. Once average data were calculated per slide an additional calculation provided a mean vector and circular standard deviation for each animal (3 slides per animal). These values were used to perform the Watson-Williams F-Test. After all averages were collected for each animal, data were merged to get one grand mean vector and one circular standard deviation for both the wild-type mice and the CD44 knockout mice. In addition, an F-ratio was calculated to determine whether the variance in the CD44 knockout mice was different than the wild-type using Data Desk software.

Additionally, in order to ensure measurement reliability, an error test containing at least 25 measurements was performed prior to data analysis according to the Dahlberg formula described by Harris et al. (2009). The calculated error for 33 data points equaled 1.4 indicating that differences in measurement larger than 1.4º are determined to be reliable.

$$d = \sqrt{\frac{\sum_{i=1}^{n} (X_{1i} - X_{2i})^2}{2n}}$$

Figure 15: Dahlberg's Formula (Harris et al., 2009).

CHAPTER IV: Results and Discussion

Results

Specific Aim One

Wild-type fibroblast measurements ranged from 79.7º to 129.3º with average vectors ranging from 89.4º to 115.7º among the different slides (Table 1). Refer to appendix A for full data set.

Table 1: Results for Wild-type PDL Development Analysis

Specimen	Slide	Average of Angles Measured	Mean Vector	Circular Standard Deviation
WT 1	38.2	110.042º	112.4º	2.4º
	39.1	115.694º		
	39.2	111.569		
WT 2	41.2	102.068º	96.6º	5.3º
	42.1	89.422º		
	42.2	98.381º		
WT 3	42.1	89.891º	90.9º	1.5º
	42.2	89.757º		
	43.1	93.033º		
WT 4	13.1	95.286º	105.1º	7.3º
	14.1	112.642º		
	14.3	107.435º		

CD44 knockout fibroblast measurements ranged from 85.1º to 138.9º with average vectors ranging from 92.1º to 116.4º (Table 2). Refer to appendix B for full data set.

Table 2: Results for CD44 Knockout PDL Development Analysis

Specimen	Slide	Average of Angles Measured	Mean Vector	Circular Standard Deviation
KO 11	19.2	95.299º	107.3º	8.7º
	20.1	109.985º		
	20.2	116.368º		
KO 12	15.1	106.525º	99.1º	5.9º
	15.2	98.567º		
	16.1	92.109º		
KO 13	12.1	99.344º	102.0º	7.1º
	13.1	111.744º		
	13.2	95.013º		
KO 14	11.2	104.522º	106.7º	1.6º
	12.1	108.263º		
	12.2	107.265º		

The calculated p-value from the Watson-Williams F-test indicated that the difference in the angle measurements of PDL fibroblast cells among wild-type and CD44 knockout mice was not statistically significant at 41 days postnatal. Additionally, the calculated p value from the F-test showed that the variances between the wild-type and CD44 knockout animals was also not statistically significant.

Table 3: Comparative Data for PDL Development Analysis

Specimen	Mean Vector	Circular Standard Deviation	p-Value (Watson-Williams F-Test)	F-Ratio
WT	101.3º	8.2º	0.6	0.7
KO	103.8º	3.4º		

Specific Aim Two

As a whole, 27 procedures were performed in which orthodontic wires were placed on the maxilla of both wild-type and CD44 knockout mice. Throughout these procedures we learned the proper steps needed to ensure efficiency and success with this part of the study. During the first round of procedures we placed wires on 5 CD44 knockout mice. One out of the five mice died when waking up from the anesthetic. Out of the four remaining CD44 knockout mice, two had activated wires five days after the wires were placed. The second round of procedures involved four wild-type mice. Two of the four mice experienced unexpected deaths after injection of the anesthetic. After consulting the veterinarian, the remaining mice were sacrificed as it was determined that there may have been an issue with the anesthetic mixture that would have caused pain and problems for the remaining mice. In the third round of procedures seven wild-type mice were used. After the first two mice died following the injection of the anesthetic a new anesthetic mixture was prepared using a fresh saline solution. The remaining five mice survived the procedure. One of the remaining five mice died two days after wire activation. Of the four remaining mice, one had an activated wire after the five-day experimental phase. Intraperitoneal BrdU injections were performed on all four remaining mice, however two of the mice died after the BrdU injections. For the fourth and final round of procedures ten wild-type mice were used. One mouse died coming out of the anesthetic. The remaining nine mice were placed on a very strict diet of protein gel and watered down hard food. One of the remaining nine mice died three days after wire activation. After the five-day experimental phase six of the eight remaining mice had activated wires. Please refer to the table below for full inventory for this study.

Table 4: Mouse Inventory for the Orthodontic Injury Study

Round	Mouse #	Strain	Survival	Activation	Prepped	Sectioned
1	195	KO	Died	NA	NA	NA
1	194	KO	Survived	Activated	Yes	Yes
1	182	KO	Survived	Deactivated	Yes	No
1	181	KO	Survived	Deactivated	Yes	No
1	193	KO	Survived	Activated	Yes	Yes
2	123	WT	Died	NA	NA	NA
2	121	WT	Died	NA	NA	NA
2	120	WT	Died	NA	NA	NA
2	124	WT	Died	NA	NA	NA
3	NA	WT	Died	NA	NA	NA
3	NA	WT	Died	NA	NA	NA
3	152	WT	Died	NA	NA	NA
3	153	WT	Died	NA	NA	NA
3	156	WT	Died	NA	NA	NA
3	157	WT	Survived	Activated	Yes	Yes
3	154	WT	Survived	Deactivated	Yes	No
4	173	WT	Survived	Deactivated	Yes	No
4	171	WT	Survived	Activated	Yes	Yes
4	159	WT	Died	NA	NA	NA
4	172	WT	Survived	Activated	Yes	Yes
4	165	WT	Survived	Activated	Yes	Yes
4	163	WT	Died	NA	NA	NA
4	164	WT	Survived	Activated	Yes	Yes
4	166	WT	Survived	Activated	Yes	Yes
4	158	WT	Survived	Deactivated	Yes	No
4	167	WT	Survived	Activated	Yes	Yes

Discussion

Specific Aim One

The similarity in angle measurements between the wild-type and CD44 knockout animals provides some insight on what is occurring within the PDL as the teeth reach occlusion. Although it was previously determined that there is a statistically significant difference in the angle measurements of fibroblasts within the PDL of day 26 dpn wild-type and CD44 knockout animals (Boyd et al., 2010), the lack of a statistically significant difference at day 41 dpn provides an opportunity to consider alternative mechanisms at this later time point.

There are three possible explanations for these results. First, it is important to consider the possibility that the CD44 receptor is not a significant part of PDL fibroblast organization and overall PDL development at day 41 dpn. While CD44 may be active during PDL development it could be a more significant factor at different times in development as we see at day 26 dpn. The 15-day difference between day 26 and day 41 mice should be considered when analyzing the two sets of data. It is possible that impairment of the CD44 knockout mice is corrected by the time the mice reach day 41 dpn. Second, since data found in this study lie in the same range as those found in the previous study, one must consider verifying the day 26 dpn data. It is possible that the previous data set provided a false result and that PDL fibroblast angle measurement at day 26 dpn are not statistically different between the CD44 knockout mice and the wild-type controls. Lastly, further investigation into the other receptors within the PDL needs to be applied to determine whether there is a functional redundancy in CD44 knockout

mice. Due to the presence of other signal cell receptors found within the PDL it is possible that the activity of receptors other than CD44 is upregulated to compensate for the impairment of the CD44. Other hyaluronan receptors include HARE, TLR4 and RHAMM, which interact with hyaluronan as hyaladherins in order to induce the transduction of intercellular signals. RHAMM (receptor for hyaluronan-mediated motility) in particular has been closely linked to the mechanism of CD44, making it more likely to be the cause of a CD44 knockout functional redundancy. When bound to cell membranes, RHAMM interacts with hyaluronan, triggering a mechanism that leads to cytoskeletal rearrangement (Solis et al., 2011). In 2004, it was discovered that in joint inflammation, which leads to collagen-induced arthritis, RHAMM compensates for the loss of CD44 when CD44 is inactivated (Nedcetzki et al., 2004). When CD44 is inactivated RHAMM is upregulated, which supports cell migration. Due to the accumulation of hyaluronan that occurs in CD44 deficient tissue, RHAMM activates leading to mechanisms such as cell migration, differentiation, and cell proliferation. This mechanism is also possible in periodontal tissue as RHAMM is also expressed throughout the periodontium.

Specific Aim Two

Through the orthodontic procedures we were able to develop an efficient protocol that ensured a higher likelihood of wire activation after the experimental period. Between the first and second round of procedures we adjusted the restraining device in order to make sure that the mice were not harmed while restrained. After the unexpected deaths during round two we decided to prepare a new solution of the anesthetic mixture in case the previously used mixture had been contaminated. Fresh batches of anesthetic

were then prepared prior to each round of procedures. Between the second and the third procedures we continued using the changes noted above. After the deaths following the BrdU injections we noted that intraperitoneal injections given while the mice were anesthetized increased the likelihood for internal damage. Therefore, at the time of wire clipping, while mice were anesthetized, BrdU injections should be administered subcutaneously. Additionally, it was also noted that close attention to the daily weight measurements made after wire activation provided information on the activation status of wires. A typical 0.5-1.0 gram loss of weight was noticed in the first two days after wire activation most likely because of the discomfort felt from tooth movement. By day three during the experimental phase the mice began to gain weight back at a rate of approximately 0.5 grams per day. Mice that did not follow this typical pattern gained weight back at a much faster rate. Mice that followed the abnormal weight pattern during the 5-day experimental period typically had deactivated wires. In order to control for this variation it was decided that a strict soft food diet would be provided during the experimental phase. Between rounds three and four we noticed that dissecting the maxilla and cutting the tissue bilaterally made it very difficult to properly orient the tissue during the embedding process. We therefore decided to use the entire mouse skull minus the mandible for histological analysis following future procedures according to a procedure noted in a prior study of mouse maxilla (Griffiths et al., 1967).

The mandible and maxilla were used separately between the two studies depending on the accessibility of either jaw bone and its role in the experiment. For specific aim one the mandible was used because it is easier to fully dissect from the skull than the maxilla. On the other hand, the maxilla was used for specific aim two because

experimenters were better able to attach an orthodontic wire with greater stability to the upper jaw.

Conclusion

At day 41 dpn, PDL fibroblast angle measurements are not different statistically between the wild-type and CD44 knockout mice indicating that CD44 impairment does not alter the PDL organization and development in mice at day 41 dpn.

Future Studies

Specific Aim One

There are three future studies that can give further evidence to examine the role of CD44 in PDL development. In order to test whether the CD44 impairment in the knockout mice was corrected between day 26 and day 41 dpn it would be crucial to analyze the histology at various time points between day 26 and day 41. Histological analysis between day 26 and day 41 dpn could provide information as to when the CD44 impairment is corrected, if this theory is correct.

Additionally, since the CD44 knockout mice used in this study lacked the function of the CD44 receptor throughout their entire development, it would be valuable to test the response when CD44 function is impaired at a certain time during development. Knocking out CD44 function at a time point such as day 31 dpn could

provide valuable data supporting the hypothesis that CD44 is important when regulating PDL repair in response to orthodontic injury.

Finally, it would be beneficial to test these experiments with other cell receptors such as RHAMM in order to determine the level of significance that each receptors plays within the PDL.

Specific Aim Two

Further analysis is needed to determine the role of CD44 in the recruitment of fibroblasts to sites of injury for repair. Now that an efficient and successful protocol has been tested additional CD44 knockout specimens are needed for comparison to the wild-type control sections that have been collected.

BIBLIOGRAPHY

Acharya P., Majumdar S., Jacob M., Hyaden J., Mrass P., Weninger W., Assoian R., and Pure E. (2008). Fibroblast migration is mediated by CD44-dependent TGFβ activation. *Journal of Cell Science*. 121. 1393-1402.

Bajorath, Jorgen. "Molecular Organization, Structural Features, and Ligand Binding Characteristics of CD44, a Highly Variable Cell Surface Glycoprotein with Multiple Functions." *Proteins: Structure, Function, and Genetics* 39.2 (2000): 103-11.

Berkovitz, B. K. B., B. J. Moxham, and Hubert N. Newman. *The Periodontal Ligament in Health and Disease*. Oxford: Pergamon, 1982.

Boyd, T., Popowics, T. Receptor CD44 Gene Knock-out Mice Exhibit Altered PDL Development. Unpublished Data. UWSOD SURF Research Paper. 2010.

Brooks, Patricia Joyce, Dorrin Nilforoushan, Morris Frank Manolson, Craig A. Simmons, and Siew-Ging Gong. "Molecular Markers of Early Orthodontic Tooth Movement." *The Angle Orthodontist* 79.6 (2009): 1108-113.

Griffiths, D., L. Furstman, and S. Bernick. "Postnatal Development of the Mouse Palate1." *American Journal of Orthodontics* 53.10 (1967): 757-68.

"Haematoxylin Eosin (H&E) Staining | Protocols Online." *Haematoxylin Eosin (H&E) Staining | Protocols Online*. N.p., n.d. Web. 1 July 2012. <http://protocolsonline.com/histology/haematoxylin-eosin-he-staining/>.

Häkkinen L., Oksala O., Salo T., Rahemtulla F., and Larjava H. (1993). Immunohistochemical localization of proteoglycans in human peridontium. *The Journal of Histochemistry and Cytochemistry*. Vol. 41 No. 11. 1689-1699.

Harris, Edward F., and Richard N. Smith. "Accounting for Measurement Error: A Critical but Often Overlooked Process." *Archives of Oral Biology* 54 (2009): S107-117.

Huebener, Peter, Tareq Abou-Khamis, Pawel Zymek, Marcin Bujak, Xia Ying, Khaled Chatila, Sandra Haudek, Geeta Thakker, and Nikolaos G. Frangogiannis. "CD44 Is Critically Involved in Infarct Healing by Regulating the Inflammatory and Fibrotic Response." *The Journal of Immunology* 180.4 (2008): 2625-633.

Kaewsuriyathumrong, Chatri, and Kunimichi Soma. "Stress of Tooth and PDL Structure Created by Bite Force." *Bulletin of the Tokyo Medical and Dental University* 40 (1993): 217-32.

King GJ; Keeling SD; Wronski TJ: Histomorphometric study of alveolar bone turnover in orthodontic tooth movement. Bone 1991 *12:* 401-9 (1991).

Lekic, P., and C.A.G. McCulloch. "Periodontal Ligament Cell Populations: The Central Role of Fibroblasts in Creating a Unique Tissue." *The Anatomical Record* 245.2 (1996): 327-41.

Liu, Z. J. "Does Human Relaxin Accelerate Orthodontic Tooth Movement in Rats?" *Annals of the New York Academy of Sciences* 1041.1 (2005): 388-94.

Madan, Monica S., Zee J. Liu, Gao M. Gu, and Gregory J. King. "Effects of Human Relaxin on Orthodontic Tooth Movement and Periodontal Ligaments in Rats." *American Journal of Orthodontics and Dentofacial Orthopedics* 131.1 (2007): 8.e1-.e10.

Mcculloch, Christopher A. G., Predrag Lekic, and Marc D. Mckee. "Role of Physical Forces in Regulating the Form and Function of the Periodontal Ligament." *Periodontology 2000* 24.1 (2000): 56-72.

Nanci, Antonio, and Cate A. R. Ten. *Ten Cate's Oral Histology: Development, Structure, and Function.* St. Louis, MO: Mosby Elsevier, 2008.

Naor, David, Ronit Vogt Sinov, and Dvorah Ish-Shalom. "CD44: Structure, Function, and Association with the Malignant Process." *Advances in Cancer Research* (1997): 241-319.

Nedvetzki, S., E. Gonen, N. Assayag, R. Reich, R. O. Williams, R. L. Thurmond, J.-F. Huang, B. A. Neudecker, F.-S. Wang, E. A. Turley, and D. Naor. "RHAMM, a Receptor for Hyaluronan-mediated Motility, Compensates for CD44 in Inflamed CD44-knockout Mice: A Different Interpretation of Redundancy." *Proceedings of the National Academy of Sciences* 101.52 (2004): 18081-8086.

Okafuji, N., Z. Liu, and G. King. "Assessment of Cell Proliferation during Mandibular Distraction Osteogenesis in the Maturing Rat." *American Journal of Orthodontics and Dentofacial Orthopedics* 130.5 (2006): 612-21.

Ponta, Helmut, Larry Sherman, and Peter A. Herrlich. "CD44: From Adhesion Molecules to Signaling Regulators." *Nature Reviews: Molecular and Cell Biology* 4 (2003): 33-45.

Puré, Ellen, and Richard K. Assoian. "Rheostatic Signaling by CD44 and Hyaluronan." *Cellular Signaling* 21 (2009): 651-55.

Rody, Wellington J., Gregory J. King, and Gaoman Gu. "Osteoclast Recruitment to Sites of Compression in Orthodontic Tooth Movement." *American Journal of Orthodontic and Dentofacial Orthopedics* 120 (2001): 477-89.

Solis, Mairim A., Ying-Hui Chen, Tzyy Y. Wong, Vanessa Z. Bittencourt, Yen-Cheng Lin, and Lynn L.H. Huang. "Hyaluronan Regulates Cell Behavior: A Potential Niche Matrix for Stem Cells." *Biochemistry Research International* 2012 (2011): 1-11.

von Böhl, M., and A. M. Kuijpers-Jagtman. "Hyalinization during Orthodontic Tooth Movement: A Systematic Review on Tissue Reactions." *The European Journal of Orthodontics* 31.1 (2008): 30-36.

Weinreb M., Gal D., Weinreb M.M., and Pitaru S. (1997). Changes in the shape and orientation of periodontal ligament fibroblasts in the continuously erupting rat incisor following removal of the occlusal load. *Journal of Dental Research*. 76. 1660-1666.

Vora, Siddharth. "Orthodontic Tooth Movement Induced Root Resorption and Repair in ANK KO Mice." Unpublished Data. MSD Thesis Proposal (2011): 1-21.

Appendix A
Data from Wild-type Animals

Specimen	Angle 1	Angle 2	Angle 3	Angle 4	Angle 5
WT1D60Lt38.2	120.18º	114.32º	108.83º	105.57º	101.33º
WT1D60Lt39.1	116.75º	125.07º	112.48º	110.30º	113.90º
WT1D60Lt39.2	110.65º	113.05º	104.42º	100.65º	129.27º
WT2D60Rt41.2	99.73º	106.08º	96.53º	101.15º	106.85º
WT2D60Rt42.1	110.90º	105.35º	95.13º	93.78º	94.73º
WT2D60Rt42.2	99.12º	104.52º	93.02º	98.87º	96.38º
WT3D60Lt42.1	96.42º	100.20º	74.35º	97.27º	81.08º
WT3D60Lt42.2	80.33º	88.82º	98.04º	79.65º	101.97º
WT3D60Lt43.1	102.08º	92.50º	83.43º	93.20º	93.95º
WT4D60Rt13.1	99.37º	95.28º	90.88º	96.95º	93.95º
WT4D60Rt14.1	105.33º	110.17º	124.60º	120.80º	102.35º
WT4D60Rt14.3	114.87º	111.40º	103.98º	94.83º	112.02º

Specimen	Mean Vector	Circular Standard Deviation
WT1D60Lt38.2	110.042º	6.614º
WT1D60Lt39.1	115.694º	5.132º
WT1D60Lt39.2	111.569º	9.873º
WT2D60Rt41.2	102.068º	3.898º
WT2D60Rt42.1	89.422º	27.332º
WT2D60Rt42.2	98.381º	3.775º
WT3D60Lt42.1	89.891º	10.243º
WT3D60Lt42.2	89.757º	9.067º
WT3D60Lt43.1	93.033º	5.921º
WT4D60Rt13.1	95.286º	2.851º
WT4D60Rt14.1	112.642º	8.674º
WT4D60Rt14.3	107.435º	7.255º

Appendix B
Data from CD44 Knockout Animals

Specimen	Angle 1	Angle 2	Angle 3	Angle 4	Angle 5	Angle 6
Mut11D60Rt19.2	87.82º	87.60º	98.09º	98.03º	98.62º	102.87º
Mut11D60Rt20.1	109.95º	113.33º	113.12º	103.53º	NA	NA
Mut11D60Rt20.2	119.85º	117.18º	115.75º	116.33º	113.28º	115.82º
Mut12D60Rt15.1	117.05º	97.85º	104.70º	NA	NA	NA
Mut12D60Rt15.2	100.13º	95.55º	100.02º	NA	NA	NA
Mut12D60Rt16.1	85.08º	101.60º	90.90º	90.88º	NA	NA
Mut13D60Rt12.1	96.07º	93.57º	101.68º	98.83º	106.58º	NA
Mut13D60Rt13.1	99.30º	116.28º	102.77º	102.33º	138.87º	NA
Mut13D60Rt13.2	94.48º	95.23º	95.33º	NA	NA	NA
Mut14D60Rt11.2	110.98º	106.70º	95.40º	108.83º	119.63º	85.58º
Mut14D60Rt12.1	85.55º	91.62º	120.93º	112.32º	130.75º	NA
Mut14D60Rt12.2	90.47º	123.72º	110.00º	121.12º	101.73º	96.60º

Specimen	Mean Vector	Circular Standard Deviation
Mut11D60Rt19.2	95.499º	5.751º
Mut11D60Rt20.1	109.985º	3.960º
Mut11D60Rt20.2	116.368º	1.958º
Mut12D60Rt15.1	106.525º	7.954º
Mut12D60Rt15.2	98.567º	2.134º
Mut12D60Rt16.1	92.109º	5.970º
Mut13D60Rt12.1	93.344º	4.521º
Mut13D60Rt13.1	111.744º	14.72º
Mut13D60Rt13.2	95.013º	0.379º
Mut14D60Rt11.2	104.552º	11.085º
Mut14D60Rt12.1	108.263º	17.281º
Mut14D60Rt12.2	107.265º	12.259º